The Astrophysical Journal, 828:84 (10pp), 2016 September 10 doi:10.3847/0004-637X/828/2/84

POLARIZED LINE FORMATION WITH LOWER-LEVEL POLARIZATION AND PARTIAL FREQUENCY REDISTRIBUTION

H. D. Supriya[1], M. Sampoorna[1], K. N. Nagendra[1], J. O. Stenflo[2,3], and B. Ravindra[1]
[1] Indian Institute of Astrophysics, Bangalore 560034, India
[2] Institute of Astronomy, ETH Zurich, CH-8093 Zurich, Switzerland
[3] Istituto Ricerche Solari Locarno, Via Patocchi, CH-6605 Locarno-Monti, Switzerland
Received 2016 January 29; revised 2016 June 10; accepted 2016 July 5; published 2016 September 7

ABSTRACT

In the well-established theories of polarized line formation with partial frequency redistribution (PRD) for a two-level and two-term atom, it is generally assumed that the lower level of the scattering transition is unpolarized. However, the existence of unexplained spectral features in some lines of the Second Solar Spectrum points toward a need to relax this assumption. There exists a density matrix theory that accounts for the polarization of all the atomic levels, but it is based on the flat-spectrum approximation (corresponding to complete frequency redistribution). In the present paper we propose a numerical algorithm to solve the problem of polarized line formation in magnetized media, which includes both the effects of PRD and the lower level polarization (LLP) for a two-level atom. First we derive a collisionless redistribution matrix that includes the combined effects of the PRD and the LLP. We then solve the relevant transfer equation using a two-stage approach. For illustration purposes, we consider two case studies in the non-magnetic regime, namely, the $J_a = 1$, $J_b = 0$ and $J_a = J_b = 1$, where J_a and J_b represent the total angular momentum quantum numbers of the lower and upper states, respectively. Our studies show that the effects of LLP are significant only in the line core. This leads us to propose a simplified numerical approach to solve the concerned radiative transfer problem.

Key words: line: formation – methods: numerical – polarization – radiative transfer – scattering – Sun: atmosphere

1. INTRODUCTION

The linear polarization of the spectral lines is produced due to the absorption, emission, and scattering of radiation in the solar atmosphere. The anisotropic illumination of the atom induces atomic alignment, which in turn gives rise to the polarization of the radiation (scattering polarization). There are two important theoretical approaches developed so far to study the physics of scattering polarization. The first one is the self-consistent approach developed by Landi Degl'Innocenti (1983) using the density matrix formalism, starting from the principles of quantum electrodynamics. One of the main advantages of this "density matrix" approach is that it allows one to take into account the polarization of all levels of the atomic system under consideration. This naturally allows to take into account the lower level polarization (LLP). The density matrix formalism is developed under the flat spectrum approximation and hence its main limitation is the difficulty to take into account the effects of partial frequency redistribution (PRD). The second theoretical approach is the semi-classical one, which provides the advantage of including the effects of PRD by means of redistribution matrices (Stenflo 1994, hereafter S94). Using this "redistribution matrix" approach, our understanding of the physics of resonance scattering has improved greatly and the effects of PRD have been studied extensively. The limitation of this theory is that using it we can deal with only two-level and two-term atoms with unpolarized, infinitely sharp lower levels.

The many anomalous spectral structures in the Second Solar Spectrum (SSS, Stenflo & Keller 1997; Stenflo et al. 2000) cast doubt on the general assumption, made in the redistribution matrix approach, that the anisotropic illumination of atoms in the solar atmosphere induces population imbalances only in the upper level and the lower level is assumed to be unpolarized. Except for the case when the total angular momentum[4] of the lower level is $J_a = 0$ or $1/2$, the assumption of zero atomic alignment in the lower level is questionable, particularly when the lower level is different from the ground state. Trujillo Bueno & Landi Degl'Innocenti (1997) studied the influence of lower level atomic polarization on the scattering line polarization for the case of a two-level atom with $J_a = 1$ and $J_b = 0$. This is an example where the resulting polarization is completely due to the population imbalances in the sublevels of the lower atomic level. They used the density matrix approach and solved simultaneously the statistical equilibrium equations (SEEs), neglecting stimulated emission and the transfer equation under complete frequency redistribution (CRD). This theory was later applied to explain many spectral features in the SSS. Landi Degl'Innocenti (1998) introduced optical depopulation pumping of the lower levels as a possible mechanism to explain the observed linear polarization in the Na I D_1 line. Trujillo Bueno (1999) showed the importance of LLP in the case of the Mg I b_2 line. Also he pointed out the importance of the depolarizing elastic collisions and their role in decreasing the alignment of the atomic levels (see also Casini et al. 2002). Trujillo Bueno et al. (2002) demonstrated the operation of the ground-level Hanle effect and importance of the selective absorption from the ground level to the generation of the polarization in the He I triplet system. Also the importance of atomic polarization of the metastable lower level of the Ca II infrared triplet was presented by Manso Sainz & Trujillo Bueno (2003, 2010). However, in all the above-mentioned studies, except in Landi Degl'Innocenti (1998), the effects of the PRD were neglected. In Nagendra (2003) the

[4] J_a and J_b represent total angular momentum quantum numbers of the lower and upper levels, respectively.

effects of PRD on linear polarization profiles have been reviewed and the limitations of CRD approximation are pointed out (see also Nagendra 2014, 2015). It is well known that CRD approximation is sufficient in describing the line core polarization, whereas the PRD effects are important in the wings of strong resonance lines.

Formulation of a general self-consistent theory for radiative transfer problem including the effects of PRD and LLP is a complex theoretical problem. Landi Degl'Innocenti et al. (1997) have formulated a theory for coherent scattering that takes into account the LLP. This theory is based on the concept of "metalevels." Based on this theory, Belluzzi et al. (2015) have recently derived the collisionless redistribution matrix for a two-term atom with hyperfine structure splitting in the non-magnetic regime by including the polarizability of the lower hyperfine levels (F levels). They have applied this theory to the problem of Na I D lines. In their studies they have treated the LLP factor as a free parameter. Note that in the present paper we do not treat the LLP factor as a free parameter, but instead obtain it under the CRD limit for a two-level atom. Casini et al. (2014) have also presented a new quantum scattering theory with which they have derived a generalized redistribution function for a polarized two-term atom with hyperfine structure splitting. As an alternative attempt, in the present paper, we perform numerical computations for a two-level atom by combining the redistribution matrix approach and the density matrix approach. Using the redistribution matrix approach, we derive the collisionless PRD matrix (the so-called type II redistribution matrix in the nomenclature of Hummer 1962), including the effects of LLP. In the process, the density matrix elements of the lower level are appropriately incorporated in to the PRD matrix derived starting from the Kramers–Heisenberg scattering formulation. We remark that only the population imbalances among the sublevels of the lower level are taken into account, while the coherences among them are ignored. This is consistent with the assumption of an infinitely sharp lower level. The lower level density matrix elements are obtained by solving the SEEs that are derived using the density matrix approach. The type II redistribution matrix so derived is then included in the radiative transfer equation. To this end we use the quantum field theory approach given by S94 to obtain the transfer equation for the problem at hand. We further apply this theoretical formulation to the cases of $1 \rightarrow 0 \rightarrow 1$ and $1 \rightarrow 1 \rightarrow 1$ transitions in the non-magnetic regime.

In Section 2 we present the collisionless redistribution matrix for a two-level atom with PRD and LLP mechanisms properly taken into account. In Section 3 the radiative transfer equation for solving the concerned problem is presented. Section 4 concerns a discussion on the influence of LLP on the polarized line profiles formed under PRD. In Section 5 we propose a simple alternative approach to solve the same problem. The conclusions are presented in Section 6. The two-stage numerical procedure used to solve the transfer equation and SEEs is described in the Appendix.

2. REDISTRIBUTION MATRIX WITH PRD AND LLP

As a first step we have derived the redistribution matrix including the effects of PRD and LLP. We considered a general case of $J_a \rightarrow J_b \rightarrow J_a$ scattering transition. We follow the Kramers–Heisenberg approach as given in Stenflo (1998) but include the contribution from the lower level density matrix elements. In Stenflo (1998) the populations of the magnetic sublevels were assumed to be the same for all the magnetic sublevels of the lower level. We relax this assumption here and thereby take into account the population imbalances among the lower magnetic sublevels. Following the procedure given in Appendices A and B of Sampoorna et al. (2007), we express the type II redistribution matrix with LLP in terms of irreducible spherical tensors of Landi Degl'Innocenti & Landolfi (2004, hereafter LL04). After an elaborate algebra we obtain the expression for the type II redistribution matrix with LLP in the atomic frame as

$$
\begin{aligned}
\boldsymbol{R}^{\rm II}_{ij}(\xi, \boldsymbol{n}, \xi', \boldsymbol{n}', \boldsymbol{B}) = \frac{2}{3}(2J_a+1)^2 \sum_{\mu_a\mu_f\mu_b\mu_b' qq'q''q'''}
&\times \sum_{K'K''QK_LQ_L} \sqrt{(2K'+1)(2K''+1)(2K_L+1)} \\
&\times (-1)^{q''-q'}(-1)^{J_a-\mu_a}(-1)^{Q} \frac{\Gamma_R}{\Gamma_R+\Gamma_I+iQg_b\omega_L} \\
&\times \rho^{K_L}_{Q_L} \begin{pmatrix} J_a & J_a & K_L \\ \mu_a & -\mu_a & -Q_L \end{pmatrix} \begin{pmatrix} J_b & J_a & 1 \\ -\mu_b & \mu_a & -q' \end{pmatrix} \\
&\times \begin{pmatrix} J_b & J_a & 1 \\ -\mu_b & \mu_f & -q \end{pmatrix} \begin{pmatrix} J_b & J_a & 1 \\ -\mu_b' & \mu_a & -q''' \end{pmatrix} \\
&\times \begin{pmatrix} J_b & J_a & 1 \\ -\mu_b' & \mu_f & -q'' \end{pmatrix} \begin{pmatrix} 1 & 1 & K'' \\ q & -q'' & Q \end{pmatrix} \\
&\times \begin{pmatrix} 1 & 1 & K' \\ q' & -q''' & Q \end{pmatrix} \delta(\xi - \xi' - \nu_{af}) \\
&\times \frac{1}{2}[\phi(\nu_{J_b\mu_b',J_a\mu_a} - \xi') + \phi^*(\nu_{J_b\mu_b,J_a\mu_a} - \xi')] \\
&\times (-1)^{Q} T^{K''}_{Q}(i, \boldsymbol{n}) T^{K'}_{-Q}(j, \boldsymbol{n}'). \qquad (1)
\end{aligned}
$$

In the above equation μ's denote the magnetic substates of a given J-state. The multipolar components of the lower level density matrix are denoted by $\rho^{K_L}_{Q_L}$. The multipolar index $0 \leqslant K_L \leqslant 2J_a$ with $Q_L \in [-K_L, +K_L]$ is associated with the lower level having total angular momentum J_a. $\rho^{K_L}_{Q_L}$ can be obtained by solving the polarized SEEs as given in Equations (10.1) and (10.2) of LL04. SEEs given in LL04 take into account both population imbalances and coherences while the redistribution matrix derived above takes into account only the population imbalances. This is because the first $3j$ symbol which arises due to the inclusion of LLP restricts the value of Q_L to 0. All the different symbols appearing in the above equation are consistent with Sampoorna (2011), therefore we do not elaborate on them. The profile function $\phi(\nu_{J_b\mu_b,J_a\mu_a} - \xi)$ is defined in Equation (40) of Sampoorna (2011).

The above expression gives the $\boldsymbol{R}^{\rm II}$ redistribution matrix in the atomic frame for a two-level atom without hyperfine structure splitting. A more general expression for this matrix for a multiplet (including also hyperfine structure) is given in Landi Degl'Innocenti et al. (1997, see Equation (12) in their paper; see also Equation (1) in Landi Degl'Innocenti 1999).

The expression in Equation (1) is normalized to

$$\frac{2}{9}\frac{(2J_a+1)^2}{(2J_b+1)}\sum_{\mu_a\mu_b}\sum_{K_L Q_L}\sqrt{(2K_L+1)}(-1)^{J_a+\mu_a} \times \rho^{K_L}_{Q_L}\begin{pmatrix} J_a & J_a & K_L \\ \mu_a & -\mu_a & -Q_L\end{pmatrix}\begin{pmatrix} J_b & J_a & 1 \\ -\mu_b & \mu_a & -q'\end{pmatrix}^2. \quad (2)$$

In order to transform the atomic frame $\boldsymbol{R}^{\rm II}$ matrix derived in Equation (1) to the laboratory reference system, we followed Section 4 of Sampoorna (2011). This process simply involves the transformation

$$\frac{1}{2}\left[\phi(\nu_{J_b\mu_b',J_a\mu_a}-\xi')+\phi^*(\nu_{J_b\mu_b,J_a\mu_a}-\xi')\right] \times \delta(\xi-\xi'-\nu_{af}) \rightarrow h^{\rm II}_{\mu_b\mu_b'}(\mu_f\mu_a)+if^{\rm II}_{\mu_b\mu_b'}(\mu_f\mu_a)], \quad (3)$$

where $h^{\rm II}$ and $f^{\rm II}$ are the auxiliary functions which are defined in Equations (22) and (23) of Sampoorna (2011). In the next section we include the type II redistribution matrix for a two-level atom with LLP, into the radiative transfer equation.

3. RADIATIVE TRANSFER EQUATION FOR A TWO-LEVEL ATOM WITH LLP

We remark that in the density matrix approach of LL04 the transfer equation is written in terms of emission and absorption coefficients. These emission and absorption coefficients depend on the density matrix elements of the upper and lower levels respectively. On the other hand, in the redistribution matrix approach, the transfer equation for a two-level atom without LLP is written in terms of a source vector that depends on the scattering integral. The scattering integral basically contains the redistribution matrix for the problem at hand. However, the transfer equation of LL04 (which can handle a two-level atom with LLP) cannot be used for our purposes because the emission vector is not written in terms of the scattering integral involving the redistribution matrices. Therefore, we need to extend the transfer equation in the redistribution matrix approach to include the effects of LLP.

In order to derive the radiative transfer equation for a two-level atom with LLP, we follow the quantum field theory approach of S94 (see his Chapters 7 and 8). It is important to note that the theory presented in S94 is in coherency matrix formalism. These equations are now converted to Stokes vector formalism in the present paper. The notations used in the present section have the same meaning as in S94 unless specified. From Equation (8.15) of S94 the radiative transfer equation can be written as

$$\frac{dD_{\alpha\alpha'}}{ds} = -\sum_\beta[(g_{\alpha\beta}D_{\beta\alpha'}+D_{\alpha\beta}g^\dagger_{\beta\alpha'}) - (f_{\alpha\beta}D_{\beta\alpha'}+D_{\alpha\beta}f^\dagger_{\beta\alpha'})]+F_c, \quad (4)$$

where F_c represents the spontaneous emission term in the coherency matrix formalism and is given by (see also Section 8.10 of S94)

$$F_c=\frac{h\nu^3}{c^2}(f_{\alpha\alpha'}+f^\dagger_{\alpha\alpha'}) \sim \int\frac{d\Omega'}{4\pi}\int dx' \times \sum_{\mu_a}\rho_{\mu_a\mu_a}\sum_{\mu_f}\sum_{\beta\beta'}w_{\alpha\beta}\,w^*_{\alpha'\beta'}\,D_{\beta\beta'}. \quad (5)$$

The components of the $\boldsymbol{g}$ and $\boldsymbol{f}$ matrices are given by Equations (8.94) and (8.95) of S94, respectively. We have to note that in S94 the total angular momentum quantum numbers of the lower and upper levels are denoted by J_μ and J_m, respectively. However, to be consistent with the notations used in the present paper, we denote them by J_a and J_b. Further, the magnetic quantum numbers μ, μ', m, and m' of S94, respectively, are replaced by μ_a, μ_a', μ_b, and μ_b'. Also the expressions in S94 are for a general transition in a multi-level system. In Section 2 we derived the redistribution matrix for a two-level atomic system with LLP under the following assumptions: (1) we neglect the off-diagonal terms of the lower level density matrix. This means that we consider only the population imbalances in the lower level and neglect the coherences between the magnetic substates. In other words, only the $\rho_{\mu_a\mu_a}$ terms contribute to the transfer equation; (2) we consider the case of Rayleigh scattering, i.e., $J_a = J_f$. These assumptions are also taken into account while using the expressions of $g_{\alpha\alpha'}$ and $f_{\alpha\alpha'}$ in the transfer equation.

The elements of the $\boldsymbol{g}$ matrix in the first two terms of the right-hand side of Equation (4) represent radiative absorption. The $\boldsymbol{f}$ matrix elements in the first two terms in the second line represent the stimulated emission. From Equations (8.113) and (8.114) of S94 and the explanation that follows, we see that the terms inside the summation in Equation (5) can be written as a Mueller matrix $\boldsymbol{M}=\boldsymbol{TWT}^{-1}$ for the scattering of the Stokes vector $\boldsymbol{S_k}$. In this manner the spontaneous emission term can be transformed from the coherency matrix formalism to the Stokes vector formalism. This transformation has to also be applied to the absorption and stimulated emission terms in the radiative transfer Equation (4). We carried out these transformations and found that the expressions we obtained are similar to those given in Section 6.7 of LL04. Thus the radiative transfer equation in Stokes vector basis can now be written as

$$\frac{dS_k}{ds}=-\sum_{j=0}^{3}A_{kj}\,S_j+\sum_{j=0}^{3}A^S_{kj}\,S_j + \frac{h\nu}{4\pi}N_{J_a}B_{J_aJ_b}\int\frac{d\Omega'}{4\pi}\int dx'\sum_{j=0}^{3}M_{kj}S_j, \quad (6)$$

where M_{kj} are the elements of the Mueller scattering matrix, A_{kj} and A^S_{kj} are the elements of the radiative absorption and stimulated emission matrix, respectively. For the problem at hand, namely, a two-level atom with LLP, this matrix $\boldsymbol{M}$ is simply the type II redistribution matrix described in Section 2.

3.1. Contribution from Thermal Emission

The transfer Equation (6) derived above does not take into account the contribution from the thermal emission. Thus, the transfer equation obtained in Equation (6) represents only pure scattering. For practical applications, however, we need to take into account the contribution from the thermal emission. For this purpose we follow the procedure given in Section 6.9 of S94 to calculate the contribution from thermal emission. Thermal emission is nothing but a limiting case in which the scattering atom has completely lost its memory about how it was excited (see Stenflo 1998). Hereafter we neglect the contribution from the stimulated emission (the second term on the right-hand side of Equation (6)). The radiative transfer

equation including the contribution from thermal emission ($j_k^{\rm thermal}$) can be written as

$$\frac{dS_k}{ds} = -\sum_{j=0}^{3} A_{kj}\, S_j + \frac{h\nu}{4\pi} N_{J_a} B_{J_a J_b} \int \frac{d\Omega'}{4\pi} \int dx' \times \sum_{j=0}^{3} R_{kj}^{\rm II} S_j + j_k^{\rm thermal}. \quad (7)$$

Generally, the thermal emission is given by the absorption matrix times the Planck function (B_{ν_o}). However, for the problem at hand, it is necessary to distinguish the processes of absorption and thermal emission. While the LLP is relevant for radiative absorption it is irrelevant for the thermal emission. Therefore, to distinguish these two processes we define the emission profile matrix as $\mathbf{\Phi}^{\rm emi}$ and absorption profile matrix as $\mathbf{\Phi}^{\rm abs}$. The absorption profile matrix is related to the absorption matrix $\boldsymbol{\eta}^A$ derived starting from the quantum field theory of S94 through

$$\boldsymbol{\eta}^A = k_L \mathbf{\Phi}^{\rm abs}, \quad (8)$$

where k_L is the line-averaged absorption coefficient (for the case when stimulated emission is neglected) defined as

$$k_L = \frac{h\nu}{4\pi} N_{J_a} B_{J_a J_b}. \quad (9)$$

The expression of the absorption profile matrix $\mathbf{\Phi}^{\rm abs}$ in the atmospheric reference frame is the same as the expression under the summation K, Q, K_I, Q_I of Equation (7.15a) of LL04. In the line of sight reference frame, this matrix is the same as Equation (6.59) of S94, which is given by

$$\mathbf{\Phi}^{\rm abs} = \begin{pmatrix} \phi_I^{\rm abs} & \phi_Q^{\rm abs} & \phi_U^{\rm abs} & \phi_V^{\rm abs} \\ \phi_Q^{\rm abs} & \phi_I^{\rm abs} & \psi_V^{\rm abs} & -\psi_U^{\rm abs} \\ \phi_U^{\rm abs} & -\psi_V^{\rm abs} & \phi_I^{\rm abs} & \psi_Q^{\rm abs} \\ \phi_V^{\rm abs} & \psi_U^{\rm abs} & -\psi_Q^{\rm abs} & \phi_I^{\rm abs} \end{pmatrix}, \quad (10)$$

where

$$\begin{aligned} \phi_I^{\rm abs} &= \phi_\Delta^{\rm abs} \sin^2\gamma + \frac{1}{2}(\phi_+^{\rm abs} + \phi_-^{\rm abs}), \\ \phi_Q^{\rm abs} &= \phi_\Delta^{\rm abs} \sin^2\gamma \cos 2\chi, \\ \phi_U^{\rm abs} &= \phi_\Delta^{\rm abs} \sin^2\gamma \sin 2\chi, \\ \phi_V^{\rm abs} &= \frac{1}{2}(\phi_+^{\rm abs} - \phi_-^{\rm abs})\cos\gamma, \\ \phi_\Delta^{\rm abs} &= \frac{1}{2}[\phi_0^{\rm abs} - \frac{1}{2}(\phi_+^{\rm abs} + \phi_-^{\rm abs})], \end{aligned} \quad (11)$$

with the corresponding expressions for $\psi_{Q,U,V}^{\rm abs}$ where ϕ_q is replaced by ψ_q, the anomalous dispersion profile. In the above expressions γ and χ denote the inclination and azimuth of the magnetic field with respect to the line of sight. Since the transfer equation is solved in the frame where the z-axis is along the atmospheric normal, we need to convert the angles γ and χ in the line-of-sight frame to the atmospheric reference frame. This can be done following Appendix B of Anusha et al. (2011). The expression for $\phi_q^{\rm abs}$ is given by (see Equation (6.52) of S94)

$$\phi_q^{\rm abs} = \frac{N(2J_a+1)}{N_{J_a}\sqrt{\pi}\Delta\nu_D} \sum_{\mu_a\mu_b} \rho_{\mu_a\mu_a} S_q(\mu_a, \mu_b) H_q. \quad (12)$$

In Equation (12) the contribution from the population imbalances in the lower level to the absorption processes is included via the density matrix element $\rho_{\mu_a\mu_a}$. The transition strength $S_q(\mu_a, \mu_b)$ is given by (see Equation (6.33) of S94)

$$S_q(\mu_a, \mu_b) = 3 \begin{pmatrix} J_a & J_b & 1 \\ -\mu_a & \mu_b & q \end{pmatrix}^2. \quad (13)$$

In the case of thermal emission, the emission processes are independent of the absorption. Therefore, we define a separate profile matrix ($\mathbf{\Phi}^{\rm emi}$) to account for the emission processes. The matrix elements of the $\mathbf{\Phi}^{\rm emi}$ matrix are now independent of the population imbalances in the lower level. The expression for $\phi_q^{\rm emi}$ is given by (see Equation (6.37) of S94)

$$\phi_q^{\rm emi} = \frac{1}{\sqrt{\pi}\Delta\nu_D} \sum_{\mu_a\mu_b} S_q(\mu_a, \mu_b) H_q. \quad (14)$$

The form of the emission profile matrix $\mathbf{\Phi}^{\rm emi}$ is the same as the absorption profile matrix $\mathbf{\Phi}^{\rm abs}$ with the elements $\phi_{I,Q,U,V,\Delta}^{\rm abs}$ replaced by $\phi_{I,Q,U,V,\Delta}^{\rm emi}$. For the problem at hand, the thermal emission term is given by

$$\boldsymbol{j}^{\rm thermal} = k_L(1-\alpha) S_{ba}\, \mathbf{\Phi}^{\rm emi} \mathbf{1}, \quad (15)$$

where $\mathbf{1} = (1,\ 0,\ 0,\ 0)^{\rm T}$ and α is the fraction of the scattering process given by

$$\alpha = \frac{N_{J_a} B_{J_a J_b} \int \phi_x J_x dx}{N_{J_a} B_{J_a J_b} \int \phi_x J_x dx + N_{J_a} C_{J_a J_b}}, \quad (16)$$

with ϕ_x the area normalized profile function which is equal to $\phi_q^{\rm emi}$ when $q = 0$. The line source function S_{ba} takes the following simple form when stimulated emission is neglected:

$$S_{ba} = \frac{N_{J_b} A_{J_b J_a}}{N_{J_a} B_{J_a J_b}}. \quad (17)$$

In the above equations, $A_{J_b J_a}$ and $B_{J_a J_b}$ are the Einstein coefficients for the spontaneous emission and absorption respectively, and $C_{J_a J_b}$ is the upward inelastic collisional rate. By defining $d\tau = -k_L ds$ we can rewrite the transfer Equation (7) including the unpolarized continuum as

$$\frac{d\boldsymbol{I}}{d\tau} = (\mathbf{\Phi}^{\rm abs} + r\boldsymbol{E})\boldsymbol{I} - (rB_{\nu_0}\mathbf{1} + \boldsymbol{S}_{\rm scatt}) - (1-\alpha) S_{ba}\, \mathbf{\Phi}^{\rm emi}\, \mathbf{1}, \quad (18)$$

where $\boldsymbol{I} = [S_0, S_1, S_2, S_3]^{\rm T} = [I, Q, U, V]^{\rm T}$, r is the ratio of continuum to line-averaged opacity, and $\boldsymbol{E}$ is a 4×4 unit matrix. The scattering source vector $\boldsymbol{S}_{\rm scatt}$ is given by

$$\boldsymbol{S}_{\rm scatt} = \int \frac{d\Omega'}{4\pi} \int dx' \boldsymbol{R}^{\rm II}(x, \boldsymbol{n}, x', \boldsymbol{n}', \boldsymbol{B}) \boldsymbol{I}(x', n'). \quad (19)$$

The above equations take a simpler form in the absence of magnetic fields. These equations are given in the next section. Furthermore, the equations presented in the present paper are for the case without elastic collisions. When elastic collisions

are included the contribution from the incoherent scattering processes to the source vector should also be taken into account. The details regarding this can be found in Sections 5.17 and 6.9 of S94.

3.2. The Non-magnetic Case

To numerically solve the problem of polarized radiative transfer including the effects of LLP, we restrict our attention to the non-magnetic case. For this particular case the Stokes V is zero, and for the planar geometry Stokes U is zero. Therefore the dimension of the problem reduces from 4×4 to 2×2. The emission profile matrix $\mathbf{\Phi}^{\rm emi}$ which contributes to the thermal emission can be simplified further for this case. In the absence of magnetic field, Equation (14) reduces to

$$\phi_q^{\rm emi} = \frac{H}{\sqrt{\pi}\Delta\nu_D} = \phi_x. \tag{20}$$

Therefore, $\phi_\Delta^{\rm emi} = 0$ (cf. Equation (11)). Thus $\phi_I^{\rm emi}$ is the only non-zero term in the emission profile matrix $\mathbf{\Phi}^{\rm emi}$, which takes the form

$$\mathbf{\Phi}^{\rm emi} = \begin{pmatrix} \phi_I^{\rm emi} & 0 \\ 0 & \phi_I^{\rm emi} \end{pmatrix}. \tag{21}$$

From Equations (15) and (21) we see that the thermal emission contributes only to the Stokes I. Equation (18) can thus be rewritten as

$$\frac{d\boldsymbol{I}}{d\tau} = \boldsymbol{K}\boldsymbol{I} - [rB_{\nu_0}\mathbf{1} + \boldsymbol{S}_l], \tag{22}$$

where $\boldsymbol{K} = \mathbf{\Phi}^{\rm abs} + r\boldsymbol{E}$. The elements of the line source vector $\boldsymbol{S}_l = (S_{I,l}, S_{Q,l})^{\rm T}$ can be written as

$$\begin{aligned} S_{I,l} &= \frac{1}{2}\int d\mu' \int dx' [R_{00}^{\rm II}(x, \mu, x', \mu') I(x', \mu') \\ &\quad + R_{01}^{\rm II}(x, \mu, x', \mu') Q(x', \mu')] + (1-\alpha) S_{ba}\, \phi_I^{\rm emi}, \\ S_{Q,l} &= \frac{1}{2}\int d\mu' \int dx' [R_{10}^{\rm II}(x, \mu, x', \mu') I(x', \mu') \\ &\quad + R_{11}^{\rm II}(x, \mu, x', \mu') Q(x', \mu')]. \end{aligned} \tag{23}$$

To solve the problem of polarized line formation including PRD and LLP, we follow a two-stage approach. In the first stage we solve the SEEs and the transfer equation simultaneously for a given J_a and J_b, taking into account the effects of the polarization of the lower level but in the limit of CRD. The density matrix elements obtained as output from the first stage are used as input to compute the redistribution matrix that enters the second stage (cf. Equation (23)). In the second stage we solve the radiative transfer equation (see Equation (22)) including the effects of PRD and LLP. Further details on the numerical method adopted are described in the Appendix. In this two-stage approach, the density matrix elements are computed neglecting the effects of PRD, and they are kept fixed when computing the polarized PRD line profiles. Such a two-stage approach is basically an approximation proposed in this paper, which lacks a complete, self-consistent theory for the problem at hand.

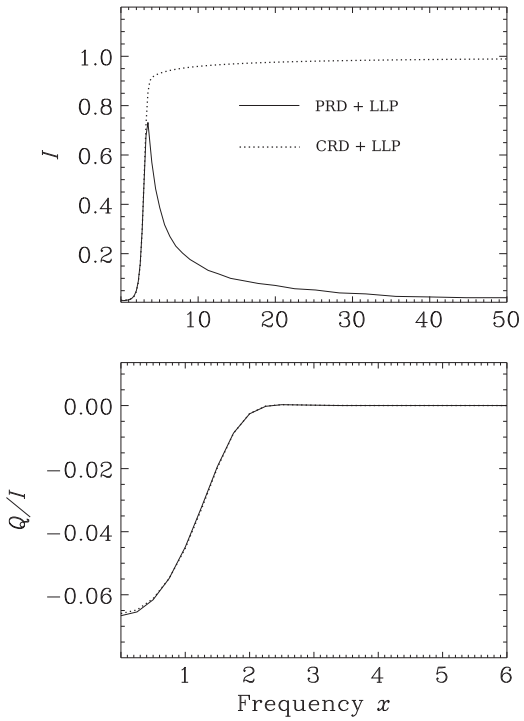

Figure 1. Emergent intensity and polarization for $\mu = 0.11$ computed using the two-stage approach. The case of the $1 \rightarrow 0 \rightarrow 1$ transition is considered with the effects of LLP. Solid line represents the case of PRD and the dotted line that of CRD. Other input parameters are $A_{J_bJ_a} = 10^8\ {\rm s}^{-1}$; $C_{J_bJ_a} = 10^4\ {\rm s}^{-1}$. No background continuum opacity is used.

4. NUMERICAL RESULTS IN THE ABSENCE OF MAGNETIC FIELDS

For our studies we consider two cases namely $J_a = 1, J_b = 0$ and $J_a = J_b = 1$ to illustrate the effects of LLP on the polarized line formation. The governing equations and the concerned numerical method of solution are described for the $J_a = J_b = 1$ case in Appendix. A similar procedure can be followed for deriving corresponding expressions for the $J_a = 1, J_b = 0$ case (see also Trujillo Bueno & Landi Degl'Innocenti 1997). For our computations, we have considered a plane parallel isothermal atmospheric slab with effective temperature of 6000 K with no incident radiation at the boundaries. Background continuum opacity is assumed to be zero. For all the results presented in this paper we consider a thick slab of total line center optical thickness $T = 10^{12}$. The effect of depolarizing elastic collisions is neglected.

4.1. The Case of the $1 \rightarrow 0 \rightarrow 1$ Transition

We consider a two-level atom with $J_a = 1$ and $J_b = 0$. The concerned SEEs and the transfer equations are given in Trujillo Bueno & Landi Degl'Innocenti (1997). Because of the cylindrical symmetry of the problem, only three density matrix elements are needed to fully specify the excitation state of the atoms, namely, $\rho^0_0(a)$, $\rho^0_0(b)$, and $\rho^2_0(a)$. For this particular case we consider the example of a hypothetical line at 5000 Å whose Einstein coefficient for spontaneous emission is $A_{ba} = 10^8\ {\rm s}^{-1}$ and whose downward inelastic collisional rate is $C_{ba} = 10^4\ {\rm s}^{-1}$.

Figure 1 shows the emergent $(I, Q/I)$ at $\mu = 0.11$ for the $1 \rightarrow 0 \rightarrow 1$ transition. Here we compare the results obtained under the limits of PRD and CRD when LLP is taken into

account. We see that the intensity profiles show the typical signatures of the PRD and CRD mechanisms. In particular, in the case of CRD we obtain an absorption line (see dotted line in Figure 1), while in the case of PRD we obtain a self-absorbed emission line (see solid line in Figure 1). The self-absorbed emission type profiles in the intensity appear because of the nature of the collisionless redistribution function exhibiting a transition from the CRD-like behavior in the line core to the coherent scattering-like behavior in the line wings (see e.g., Figure 4(a) of Rees & Saliba 1982). The Q/I profiles are identical for the PRD and CRD limits. This is because, for this particular transition in the non-magnetic regime, only the elements $R^{\rm II}_{00}$ and $R^{\rm II}_{01}$ of the redistribution matrix are non-zero and all the other elements are zero. Hence the line source vector corresponding to the polarization ($S_{Q,l}$) is always zero (see Equation (23)). This implies that the contribution to the emitted polarization for this case does not come from the redistribution processes but only from the dichroic absorption (see Trujillo Bueno & Landi Degl'Innocenti 1997). In order to understand the combined effects of PRD and LLP in a better way, we consider another case study with $J_a = J_b = 1$.

4.2. The Case of the $1 \rightarrow 1 \rightarrow 1$ Transition

For the case when $J_a = J_b = 1$, even in the absence of LLP, since the upper level is polarized, a finite amount of emergent polarization is generated unlike the case of $J_a = 1$, $J_b = 0$. For all the computations of this particular transition ($J_a = J_b = 1$), we again consider the hypothetical case like that described for $J_a = 1$, $J_b = 0$. In this case, there are four density matrix elements to be determined, namely, $\rho^0_0(a)$, $\rho^2_0(a)$, $\rho^0_0(b)$, and $\rho^2_0(b)$, when polarizability of both levels are taken into account.

Figure 2 shows the emergent (I, Q/I) at $\mu = 0.11$ for the $1 \rightarrow 1 \rightarrow 1$ transition. The solid line in Figure 2 represents the emergent profiles obtained when both the effects of PRD and LLP are considered. In order to see the importance of both effects we have overplotted the (I, Q/I) profiles obtained when only the effects of PRD are considered with an unpolarized lower level (ULL—dashed line); when the effects of LLP is considered in the limit of CRD (dotted line); and the case where only the CRD effects are considered with ULL (dotted–dashed line). Figure 2 clearly shows that the LLP effects appear only in the emergent polarization and the intensity profiles remain unchanged whether or not LLP is taken into account. We see that the LLP effects in the emergent Q/I are significant mainly in the core (up to ~2 Doppler widths, see inset in the lower panel of Figure 2), and in the wings the effects of PRD are dominant (compare solid and dashed lines). The enhancement in the emergent polarization at the line center when LLP is included is around 5%.

In the first stage of the two-stage approach, the SEEs are solved under the approximation of CRD, and thus all the transition rates that enter into the SEEs are frequency-integrated quantities. Therefore, all the redistribution effects are integrated away. The contributions to the frequency-integrated scattering probability come almost entirely from the Doppler core. In SEEs, we compare the individual transition rates for a given radiation field. For each individual transition, the contributions of the wing photons are insignificant compared with the core photons. Since it is only the core photons that are relevant to SEEs, the effects of LLP only show up in the core but are absent in the wings. We cannot exclude that the absence of LLP effects in the wings could be due to the two-stage approach that we have used. This possibility needs to be tested based on a more elaborate theory of PRD, like the recent formulations by Casini et al. (2014) and Bommier (2016).

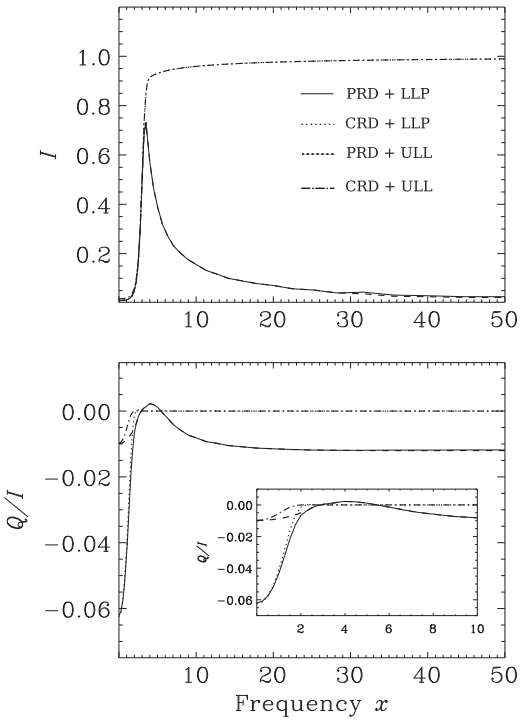

Figure 2. Emergent intensity and polarization for $\mu = 0.11$ computed using the two-stage approach for the $1 \rightarrow 1 \rightarrow 1$ case. The different line types correspond to: solid line—PRD + LLP, dotted line—CRD + LLP, dashed line—PRD + ULL, and the dotted–dashed line—CRD + ULL. The abbreviation ULL stands for unpolarized lower level. Other input parameters are $A_{J_bJ_a} = 10^8\ {\rm s}^{-1}$; $C_{J_bJ_a} = 10^4\ {\rm s}^{-1}$. No background continuum opacity is used. The inset in the Q/I panel shows the Q/I profiles for a shorter frequency bandwidth for the sake of clarity.

5. AN ALTERNATIVE APPROACH TO INCLUDE THE EFFECTS OF LLP IN POLARIZED LINES FORMED UNDER PRD

The conclusion that LLP effects are only significant in the line core allows us to use an alternative approach to solve the problem at hand. We refer to this approach as the correction method. In this method, we compute the line profiles taking into account PRD and neglecting LLP (in the standard two-level approach) and later apply to it the corrections due to the effects of LLP computed using the density matrix approach with CRD. The actual procedure is described below.

(i) We solve the SEEs and the transfer equation simultaneously for a given J_a and J_b, taking into account the effects of a polarized lower level in the limit of CRD. For this purpose, we use the relevant equations derived from the density matrix approach. We also neglect the stimulated emission. The Stokes Q parameter obtained through a simultaneous solution of SEEs and the polarized transfer equation is denoted by $Q^{\rm LLP}_{\rm CRD}$. For the numerical solution of this problem, we use the Rybicki and Hummer method (see Rybicki & Hummer 1991) appropriately generalized to handle the polarized lower level. The governing equations and the details of the numerical procedure followed are described in Appendix A.1.

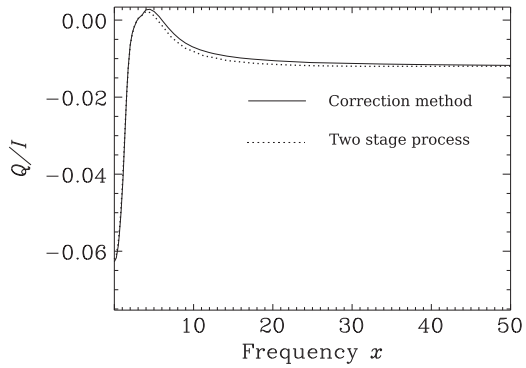

Figure 3. Emergent polarization for $\mu = 0.11$ computed using the correction method (solid line) and the two-stage approach (dotted line). Other parameters are the same as in Figure 2.

(ii) We solve the same problem as above, but now neglecting the effects of LLP. The resulting Stokes Q parameter is denoted by $Q_{\rm CRD}^{\rm ULL}$.

(iii) The difference between the solutions obtained with and without the effects of LLP is

$$\Delta Q_{\rm CRD} = Q_{\rm CRD}^{\rm LLP} - Q_{\rm CRD}^{\rm ULL}. \quad (24)$$

We refer to $\Delta\ Q_{\rm CRD}$ as the correction term.

(iv) We now solve the transfer equation for the atomic system under consideration using the standard two-level atom approach including PRD. For this purpose we use a polarized approximate lambda iteration method (Nagendra et al. 1999). The polarization thus obtained is referred to as $Q_{\rm PRD}^{\rm ULL}$.

(v) It is well known that the effects of PRD are noticeable mainly in the line wings. Our studies showed that the effects of a polarized lower level of an atomic system are confined to the line core region (see Figure 2). To a good approximation a solution including the effects of PRD and also the LLP can be obtained from

$$Q_{\rm PRD}^{\rm LLP} = Q_{\rm PRD}^{\rm ULL} + \Delta Q_{\rm CRD}. \quad (25)$$

In Figure 3 we compare the Q/I profiles obtained using the simple correction method described above and the elaborate two-stage approach proposed in this paper (see Appendix). We see that the results from both methods match closely. Thus in order to simplify the computational efforts one can use the simple correction method instead of the two-stage approach.

6. CONCLUSIONS

In this paper we have presented a numerical algorithm to solve the polarized radiative transfer problem including the effects of PRD and LLP in the general case of magnetic media. Following the Kramers–Heisenberg approach as given in Stenflo (1998), we have derived the general collisionless redistribution matrix including the effects of LLP for a two-level atomic system. This redistribution matrix now depends on the density matrix elements of the lower atomic level. We then include this redistribution matrix in the transfer equation. For this purpose, we followed the quantum field theory approach of S94.

A two-stage approach is proposed to solve the polarized radiative transfer problem including the effects of PRD and LLP in the non-magnetic regime. In the first stage we solve the SEEs and the transfer equation simultaneously under the flat spectrum approximation using the density matrix formalism developed by Landi Degl'Innocenti (1983). The density matrix elements thus obtained from the first stage are used as inputs to the second stage to compute the collisionless redistribution matrix elements. In the second stage, we use the DELOPAR method to obtain the formal solution. Furthermore, we use the frequency-angle-by-frequency-angle (FABFA) method to compute the source vector corrections.

To demonstrate the effects of PRD and LLP, we consider two examples, namely, the $1 \rightarrow 0 \rightarrow 1$ transition and $1 \rightarrow 1 \rightarrow 1$ transition. The case of the $1 \rightarrow 0 \rightarrow 1$ transition does not show any signatures of PRD in the emergent polarization profile. This is because in this particular case, the contribution to the emergent linear polarization does not come from the scattering processes but only from the dichroic absorption from the lower level. However, in the $1 \rightarrow 1 \rightarrow 1$ transition, the PRD signatures in the emergent polarization profile can be clearly seen in the line wings. Our studies indicate that the LLP effects are confined mostly to the line core region. The reason behind this appears to be that the SEEs are solved under the flat spectrum approximation, which makes the concerned transition rates frequency-integrated quantities. This leads us to a computationally simpler numerical approach called the "correction method" to study the effects of PRD and LLP on polarized line formation. We have verified that this computationally simpler correction method represents a sufficiently good approximation and is therefore useful in practical model calculations.

APPENDIX
NUMERICAL METHOD: TWO-STAGE APPROACH

In this section we describe the two-stage approach to solve the problem of polarized line formation including LLP and PRD for the non-magnetic case. In the first stage we solve the polarized SEEs and transfer equation simultaneously in the limit of CRD. For the numerical solution of this problem, we use the Rybicki and Hummer method (see Rybicki & Hummer 1991) appropriately generalized to handle polarized lower level (see also Trujillo Bueno 2003). In the second stage, we solve the polarized radiative transfer equation including the effects of LLP (through the density matrix elements derived in the first stage) and PRD.

A.1. Stage 1 of the Two-stage Approach

The governing equations and concerned numerical method for the simultaneous solution of the SEEs and transfer equation in the limit of CRD is illustrated here for the $1 \rightarrow 1 \rightarrow 1$ transition. For this particular transition, the SEEs and transfer equations are given in Trujillo Bueno (1999). There are four density matrix elements to be determined, namely, $\rho^0_0(a)$, $\rho^2_0(a)$, $\rho^0_0(b)$, and $\rho^2_0(b)$ when polarizability of both the levels are taken into account for this case. The SEEs to be solved correspond to the $K = 0$ and 2 components of the upper level, the $K = 2$ component of the lower level density matrix, and the number conservation equation. These equations can be derived starting from the general Equations (10.4) given in LL04. The upward and downward inelastic collisional rates are taken into account when solving the SEEs. J^0_0 and J^2_0 are two quantities related to the radiation field that enter the SEEs and the expressions for these are given in Trujillo Bueno (1999). The coupled transfer equations for the Stokes parameters I and Q

are given by

$$dI/ds = \epsilon_I - \eta_I^A I - \eta_Q^A Q, \tag{26}$$

$$dQ/ds = \epsilon_Q - \eta_Q^A I - \eta_I^A Q. \tag{27}$$

Here s is the geometrical distance along the ray. In the preceding equations, ϵ_I and ϵ_Q are the emission coefficients and η_I^A and η_Q^A are the absorption coefficients. They depend on the atomic density matrix elements, which in turn depend on the Stokes I and Q parameters. Thus the problem becomes both nonlinear and nonlocal. This is referred to as the NLTE problem of the second kind (see LL04). To solve this problem, we use an iterative technique based on the approximate lambda iteration (ALI) method. We note that $\epsilon_Q \neq 0$ in the case of the $1 \rightarrow 1 \rightarrow 1$ transition, whereas it is equal to 0 in the case of the $1 \rightarrow 0 \rightarrow 1$ transition as the upper level with $J_b = 0$ cannot lead to the emission of polarized radiation. The coupled transfer Equations (26) and (27) can be decoupled by working with $I_+ = I + Q$ and $I_- = I - Q$ (see Trujillo Bueno 2003). The decoupled transfer equations can be written as

$$\frac{dI_+}{ds} = \epsilon_+ - \eta_+ I_+, \tag{28}$$

$$\frac{dI_-}{ds} = \epsilon_- - \eta_- I_-, \tag{29}$$

where $\epsilon_+ = \epsilon_I + \epsilon_Q$; $\epsilon_- = \epsilon_I - \epsilon_Q$; $\eta_+ = \eta_I + \eta_Q$ and $\eta_- = \eta_I - \eta_Q$. Thus we can write the source functions S_+ and S_- as

$$S_+ = \frac{\epsilon_+}{\eta_+} = \frac{2h\nu^3}{c^2} \frac{\rho_0^0(b) - \frac{1}{4\sqrt{2}}[(3\mu^2-1)+3(\mu^2-1)]\rho_0^2(b)}{\rho_0^0(a) - \frac{1}{4\sqrt{2}}[(3\mu^2-1)+3(\mu^2-1)]\rho_0^2(a)}, \tag{30}$$

$$S_- = \frac{\epsilon_-}{\eta_-} = \frac{2h\nu^3}{c^2} \frac{\rho_0^0(b) - \frac{1}{4\sqrt{2}}[(3\mu^2-1)-3(\mu^2-1)]\rho_0^2(b)}{\rho_0^0(a) - \frac{1}{4\sqrt{2}}[(3\mu^2-1)-3(\mu^2-1)]\rho_0^2(a)}. \tag{31}$$

The formal solution of the transfer Equations (28) and (29) can be written as

$$I_+ = \Lambda_+[S_+], \tag{32}$$

$$I_- = \Lambda_-[S_-], \tag{33}$$

where Λ_+ and Λ_- are the operators that depend on the optical distances between the grid points. We use the short characteristics method (Olson & Kunasz 1987) to find the formal solution of the transfer Equations (28) and (29).

Now, in order to linearize the SEEs, we introduce the approximate operator based on the idea of operator splitting:

$$I_+ \simeq \Lambda_+[S_+] + (\Lambda_+ - \Lambda_+^*)[S_+^\dagger],$$
$$I_- \simeq \Lambda_-[S_-] + (\Lambda_- - \Lambda_-^*)[S_-^\dagger], \tag{34}$$

where the "†" represents the quantities known from the previous iteration. Following Olson et al. (1986), the approximate operators Λ_+^* and Λ_-^* are chosen to be the diagonals of the respective actual lambda operators. The radiation field tensors can now be written as

$$J_0^0 = J_0^{0,\mathrm{eff}} + (\Lambda_0^{*0} + \Lambda_2^{*0}) \frac{\rho_0^0(b)}{\rho_0^0(a)}, \tag{35}$$

$$J_0^2 = J_0^{2,eff} + (\Lambda_0^{*2} + \Lambda_2^{*2}) \frac{\rho_0^0(b)}{\rho_0^0(a)}, \tag{36}$$

where $J_0^{0,\mathrm{eff}}$ and $J_0^{2,eff}$ are given by

$$J_0^{0,\mathrm{eff}} = \frac{1}{2}\int dx\ \phi_x \int_{-1}^{1} d\mu\ \frac{1}{2} \times [(\Lambda_+ - \Lambda_+^*)[S_+^\dagger] + (\Lambda_- - \Lambda_-^*)[S_-^\dagger]], \tag{37}$$

$$J_0^{2,eff} = \frac{1}{4\sqrt{2}}\int dx\ \phi_x \int_{-1}^{1} d\mu\ \frac{1}{2} \times [((3\mu^2-1)+3(\mu^2-1))\,(\Lambda_+ - \Lambda_+^*)[S_+^\dagger] + ((3\mu^2-1)-3(\mu^2-1))\,(\Lambda_- - \Lambda_-^*)[S_-^\dagger]]. \tag{38}$$

The components of the Λ^* operator are given by

$$\Lambda_0^{*0} = \frac{1}{2}\int dx\ \phi_x \int_{-1}^{1} d\mu\ \frac{1}{2}\frac{2h\nu^3}{c^2}\Lambda_+^* \times \frac{1 - \frac{1}{4\sqrt{2}}[(3\mu^2-1)+3(\mu^2-1)][\rho_0^2(b)/\rho_0^0(b)]}{1 - \frac{1}{4\sqrt{2}}[(3\mu^2-1)+3(\mu^2-1)][\rho_0^2(a)/\rho_0^0(a)]},$$

$$\Lambda_2^{*0} = \frac{1}{2}\int dx\ \phi_x \int_{-1}^{1} d\mu\ \frac{1}{2}\frac{2h\nu^3}{c^2}\Lambda_-^* \times \frac{1 - \frac{1}{4\sqrt{2}}[(3\mu^2-1)-3(\mu^2-1)][\rho_0^2(b)/\rho_0^0(b)]}{1 - \frac{1}{4\sqrt{2}}[(3\mu^2-1)-3(\mu^2-1)][\rho_0^2(a)/\rho_0^0(a)]},$$

$$\Lambda_0^{*2} = \frac{1}{4\sqrt{2}}\int dx\ \phi_x \int_{-1}^{1} d\mu\ \frac{1}{2}\frac{2h\nu^3}{c^2} \times \Lambda_+^*[(3\mu^2-1)+3(\mu^2-1)] \times \frac{1 - \frac{1}{4\sqrt{2}}[(3\mu^2-1)+3(\mu^2-1)][\rho_0^2(b)/\rho_0^0(b)]}{1 - \frac{1}{4\sqrt{2}}[(3\mu^2-1)+3(\mu^2-1)][\rho_0^2(a)/\rho_0^0(a)]},$$

$$\Lambda_2^{*2} = \frac{1}{4\sqrt{2}}\int dx\ \phi_x \int_{-1}^{1} d\mu\ \frac{1}{2}\frac{2h\nu^3}{c^2} \times \Lambda_-^*[(3\mu^2-1)-3(\mu^2-1)] \times \frac{1 - \frac{1}{4\sqrt{2}}[(3\mu^2-1)-3(\mu^2-1)][\rho_0^2(b)/\rho_0^0(b)]}{1 - \frac{1}{4\sqrt{2}}[(3\mu^2-1)-3(\mu^2-1)][\rho_0^2(a)/\rho_0^0(a)]}. \tag{39}$$

In the computation of S_+ and S_- in the first iteration, we need the values of $\rho_0^0(a)$, $\rho_0^0(b)$, $\rho_0^2(a)$, and $\rho_0^2(b)$. These are obtained by assuming the LTE populations. First we compute the number densities of the lower level (N_{J_a}), upper level (N_{J_b}), and the total density ($N = N_{J_a} + N_{J_b}$). From this, we compute $\rho_0^0(a) = \frac{1}{\sqrt{3}}\frac{N_{J_a}}{N}$ and $\rho_0^0(b) = \frac{1}{\sqrt{3}}\frac{N_{J_b}}{N}$. We assume $\rho_0^2(a) = \rho_0^2(b) = 0$ in the first iteration. Preconditioning the quantity $\rho_0^0(b)/\rho_0^0(a)$, we can linearize the SEEs to obtain the

linearized equations

$$[B_{J_aJ_b}J_0^{0,\mathrm{eff}} + C_{J_aJ_b}]\rho_0^0(a) + [B_{J_aJ_b}(\Lambda^{*\,0}_0 + \Lambda^{*\,0}_2) - A_{J_bJ_a} - C_{J_bJ_a}]\rho_0^0(b) - \left[\frac{1}{2}B_{J_aJ_b}J_0^{2,eff} + \frac{1}{2}B_{J_aJ_b}(\Lambda^{*\,2}_0 + \Lambda^{*\,2}_2)\left(\frac{\rho_0^0(b)}{\rho_0^0(a)}\right)^{\dagger}\right]\rho_0^2(a) = 0, \quad (40a)$$

$$\left[-\frac{B_{J_aJ_b}}{2}J_0^{2,eff}\right]\rho_0^0(a) - \left[\frac{B_{J_aJ_b}}{2}(\Lambda^{*\,2}_0 + \Lambda^{*\,2}_2)\right]\rho_0^0(b) + \left[C^{(2)}_{J_aJ_b} - \frac{B_{J_aJ_b}}{2}J_0^{0,\mathrm{eff}} - \frac{B_{J_aJ_b}}{2}(\Lambda^{*\,0}_0 + \Lambda^{*\,0}_2) \times \left(\frac{\rho_0^0(b)}{\rho_0^0(a)}\right)^{\dagger} - \frac{B_{J_aJ_b}}{\sqrt{2}}J_0^{2,eff} - \frac{B_{J_aJ_b}}{\sqrt{2}}(\Lambda^{*\,2}_0 + \Lambda^{*\,2}_2) \times \left(\frac{\rho_0^0(b)}{\rho_0^0(a)}\right)^{\dagger}\right]\rho_0^2(a) + [C_{J_bJ_a} - A_{J_bJ_a}]\rho_0^2(b) = 0, \quad (40b)$$

$$[B_{J_aJ_b}J_0^{2,eff}]\rho_0^0(a) + [B_{J_aJ_b}(\Lambda^{*\,2}_0 + \Lambda^{*\,2}_2)]\rho_0^0(b) - \left[2B_{J_aJ_b}J_0^{0,\mathrm{eff}} + 2B_{J_aJ_b}(\Lambda^{*\,0}_0 + \Lambda^{*\,0}_2)\left(\frac{\rho_0^0(b)}{\rho_0^0(a)}\right)^{\dagger} + \frac{B_{J_aJ_b}}{\sqrt{2}}(\Lambda^{*\,2}_0 + \Lambda^{*\,2}_2)\left(\frac{\rho_0^0(b)}{\rho_0^0(a)}\right)^{\dagger} + 2C_{J_aJ_b}\right]\rho_0^2(a) + [2C^{(2)}_{J_bJ_a} - A_{J_bJ_a}]\rho_0^2(b) = 0. \quad (40c)$$

Here $C_{J_bJ_a}$ is the downward inelastic collisional rate. In the present case there is a contribution from the $K = 2$ multipole component of the inelastic collision rates, namely, $C^{(2)}_{J_aJ_b}$ and $C^{(2)}_{J_bJ_a}$. The relation between the Kth multipole component and zeroth component of different collision rates is given in Appendix 4 of LL04. Using that relation we get $C^{(2)}_{J_aJ_b} = -C_{J_aJ_b}/2$ and $C^{(2)}_{J_bJ_a} = -C_{J_bJ_a}/2$ for the $1 \rightarrow 1 \rightarrow 1$ transition (we have taken $\widetilde{K} = 1$). The above equations are then solved for the density matrix elements $\rho_0^0(a)$, $\rho_0^0(b)$, $\rho_0^2(a)$, and $\rho_0^2(b)$. In the subsequent iterations the source functions and the quantities J_0^0 and J_0^2 are updated. The iteration sequence is continued until convergence is obtained over the density matrix elements. In this way the SEEs and the transfer equations are solved simultaneously using the ALI method. The limit of ULL is recovered by setting $\rho_0^2(a)$ to zero in the above equations. It has to be noted that the time evolution equation of the lower level will then be given by $\rho^K_Q(a) = \delta_{K0}\delta_{Q0}\rho_0^0(a)$, and therefore, the Equation (40c) will vanish. The rest of the iteration procedure remains the same, which then involves solving the SEEs for the three unknowns, namely, $\rho_0^2(b)$, $\rho_0^0(b)$, and $\rho_0^0(a)$.

A similar procedure can also be followed for the case of $J_a = 1$ and $J_b = 0$, which is simpler compared to the $J_a = J_b = 1$ case, with only three density matrix elements to be determined. The SEEs and the transfer equation for this case ($J_a = 1$ and $J_b = 0$) in the non-magnetic regime are given in Trujillo Bueno & Landi Degl'Innocenti (1997).

A.2. Stage 2 of the Two-stage Approach

The density matrix elements obtained from the first stage described above are used to compute the elements of the redistribution matrix $\boldsymbol{R}^{\mathrm{II}}_{ij}(x, \mu, x', \mu')$ which is needed in the second stage. In this stage we solve the polarized transfer equation given in Equation (22). By defining the total optical depth $d\tau_{\mathrm{tot}} = (\phi_I^{\mathrm{abs}} + r)d\tau$ we can simplify Equation (22) as

$$\frac{d\boldsymbol{I}}{d\tau_{\mathrm{tot}}} = \boldsymbol{I} - \boldsymbol{S}_{\mathrm{eff}}. \quad (41)$$

Here, the effective source vector is

$$\boldsymbol{S}_{\mathrm{eff}} = \boldsymbol{S}_{\mathrm{tot}} - \boldsymbol{K'I}, \quad (42)$$

where we have redefined the total absorption matrix as

$$\boldsymbol{K'} = \frac{\boldsymbol{K}}{\phi_I^{\mathrm{abs}} + r} - \boldsymbol{E}. \quad (43)$$

The total source vector is defined as

$$\boldsymbol{S}_{\mathrm{tot}} = \frac{1}{\phi_I^{\mathrm{abs}} + r}[rB_{\nu_0}\boldsymbol{1} + \boldsymbol{S}_l]. \quad (44)$$

With these expressions we can apply the same steps as in Equations (19)–(26) of Sampoorna et al. (2008) to obtain the formal solution of the transfer equation using the DELOPAR method (see also Trujillo Bueno 2003). The transfer Equation (41) is solved iteratively using an ALI method. To compute the source vector corrections, we use the so-called FABFA method, similar to that given in Sampoorna et al. (2011). Hereon the dependencies over x and μ appear as subscripts. The formal solution of the transfer Equation (41) can be written as

$$\boldsymbol{I}_{x\mu} = \boldsymbol{\Lambda}_{x\mu}[\boldsymbol{S}_{\mathrm{tot},x\mu}]. \quad (45)$$

$\boldsymbol{\Lambda}_{x\mu}$ is the frequency- and angle-dependent integral operator, which can be split as

$$\boldsymbol{\Lambda}_{x\mu} = \boldsymbol{\Lambda}^*_{x\mu} + (\boldsymbol{\Lambda}_{x\mu} - \boldsymbol{\Lambda}^*_{x\mu}), \quad (46)$$

where $\boldsymbol{\Lambda}^*_{x\mu}$ represents the diagonal approximate operator. Now we can write the total source vector as

$$\boldsymbol{S}^{n+1}_{\mathrm{tot},x\mu} = \boldsymbol{S}^n_{\mathrm{tot},x\mu} + \delta\boldsymbol{S}^n_{\mathrm{tot},x\mu}. \quad (47)$$

Here n represents the iteration index. Using Equations (23), (44), (46), and (47) we obtain

$$\delta\boldsymbol{S}^n_{\mathrm{tot},x\mu} - p_{x\mu}\frac{1}{2}\int d\mu'\int dx'\frac{\boldsymbol{R}^{\mathrm{II}}_{x\mu,x'\mu'}}{\phi_x}\boldsymbol{\Lambda}^*_{x'\mu'}[\delta\boldsymbol{S}^n_{tot,x'\mu'}] = p_{x\mu}\overline{\boldsymbol{J}}^n_{x\mu} + p_{x\mu}(1-\alpha)\boldsymbol{1}S_{ba} + p^c_{x\mu}B_{\nu_0}\boldsymbol{1} - \boldsymbol{S}^n_{\mathrm{tot},x\mu}, \quad (48)$$

where $p_{x\mu} = \phi_x/(\phi_I^{\mathrm{abs}} + r)$ and $p^c_{x\mu} = r/(\phi_I^{\mathrm{abs}} + r)$. We have to note that in the above equation, the thermal emission term remains constant over iterations in the non-magnetic case. The mean intensity is given by

$$\overline{\boldsymbol{J}}^n_{x\mu} = \frac{1}{2}\int d\mu'\int dx'\frac{\boldsymbol{R}^{\mathrm{II}}_{x\mu,x'\mu'}}{\phi_x}\boldsymbol{I}_{x'\mu'}. \quad (49)$$

The standard steps of FABFA as given in Sampoorna et al. (2011) can now be applied to solve the system of linear equation (48) to obtain the corrections to the total source vector

($\delta \boldsymbol{S}_{\mathrm{tot},x\mu}$) in the iteration process. In this way, using the ALI method, we solve the transfer equation, which now includes the effects of PRD and LLP.

REFERENCES

Anusha, L. S., Nagendra, K. N., Bianda, M., et al. 2011, ApJ, 737, 95
Belluzzi, L., Trujillo Bueno, J., & Landi Degl'Innocenti, E. 2015, ApJ, 814, 116
Bommier, V. 2016, A&A, 591, 59
Casini, R., Landi Degl'Innocenti, E., Landolfi, M., & Trujillo Bueno, J. 2002, ApJ, 573, 864
Casini, R., Landi Degl'Innocenti, M., Manso Sainz, R., Landi Degl'Innocenti, E., & Landolfi, M. 2014, ApJ, 791, 94
Hummer, D. G. 1962, MNRAS, 125, 21
Landi Degl'Innocenti, E. 1983, SoPh, 85, 3
Landi Degl'Innocenti, E. 1999, in Solar Polarization, Vol. 243 ed. K. N. Nagendra & J. O. Stenflo (Boston, MA: Kluwer), 61
Landi Degl'Innocenti, E., Landi Degl'Innocenti, M., & Landolfi, M. 1997, in Proc. Forum THEMIS, Science with THEMIS, ed. N. Mein & S. Sahal Bŕechot (Paris: Obs. Paris-Meudon), 59
Landi Degl'Innocenti, E. 1998, Natur, 392, 256
Landi Degl'Innocenti, E., & Landolfi, M. 2004, Polarization in Spectral Lines (Dordrecht: Kluwer) (LL04)
Manso Sainz, R., & Trujillo Bueno, J. 2003, PhRvL, 91, 111102
Manso Sainz, R., & Trujillo Bueno, J. 2010, ApJ, 722, 1416
Nagendra, K. N. 2003, in ASP Conf. Proc. 288, Stellar Atmosphere Modeling, ed. I. Hubeny, D. Mihalas, & K. Werner (San Francisco, CA: ASP), 583
Nagendra, K. N. 2014, in ASP Conf. Ser., 489, Solar Polarization 7, ed. K. N. Nagendra et al. (San Francisco, CA: ASP), 179
Nagendra, K. N. 2015, in Proc. IAU Symp. 305, Polarimetry: From the Sun to Stars and Stellar Environments, ed. K. N. Nagendra et al. (Cambridge: Cambridge Univ. Press), 351
Nagendra, K. N., Paletou, F., Frisch, H., & Faurobert-Scholl, M. 1999, in Solar Polarization, Vol. 243 ed. K. N. Nagendra & J. O. Stenflo (Boston, MA: Kluwer), 127
Olson, G. L., Auer, L. H., & Buchler, J. R. 1986, JQSRT, 35, 431
Olson, G. L., & Kunasz, P. 1987, JQSRT, 38, 325
Rees, D. E., & Saliba, G. J. 1982, A&A, 115, 1
Rybicki, G. B., & Hummer, D. G. 1991, A&A, 245, 171
Sampoorna, M. 2011, ApJ, 731, 114
Sampoorna, M., Nagendra, K. N., & Frisch, H. 2011, A&A, 527, 89
Sampoorna, M., Nagendra, K. N., & Stenflo, J. O. 2007, ApJ, 670, 1485
Sampoorna, M., Nagendra, K. N., & Stenflo, J. O. 2008, ApJ, 679, 889
Stenflo, J. O. 1994, Solar Magnetic Fields: Polarized Radiation Diagnostics (Dordrecht: Kluwer) (S94)
Stenflo, J. O. 1998, A&A, 338, 301
Stenflo, J. O., & Keller, C. U. 1997, A&A, 321, 927
Stenflo, J. O., Keller, C. U., & Gandorfer, A. 2000, A&A, 355, 789
Trujillo Bueno, J. 1999, in Solar Polarization, Vol. 243 ed. K. N. Nagendra & J. O. Stenflo (Boston, MA: Kluwer), 73
Trujillo Bueno, J. 2003, in ASP Conf. Ser. 288, Stellar Atmosphere Modeling, ed. I. Hubeny, D. Mihalas, & K. Werner (San Francisco: ASP), 551
Trujillo Bueno, J., & Landi Degl'Innocenti, E. 1997, ApJL, 482, L183
Trujillo Bueno, J., Landi Degl'Innocenti, E., Collados, M., Merenda, L., & Manso Sainz, R. 2002, Natur, 415, 403